XX Polish Fluid Mechanics Conference,
Gliwice, 17-20 September 2012

AMPLITUDE MODULATED NEAR-WALL CYCLE IN A TURBULENT BOUNDARY LAYER UNDER AN ADVERSE PRESSURE GRADIENT

Artur DRÓŻDŻ, Witold ELSNER
Institute of Thermal Machinery, Czestochowa University of Technology, Poland
E-mail: arturdr@imc.pcz.czest.pl, welsner@imc.pcz.czest.pl

Abstract

The paper presents effect of amplitude modulation of small-scale turbulence by large-scale structures in a turbulent boundary layer subjected to an adverse pressure gradient. The results has been compared to the literature data for zero pressure gradient high Reynolds number cases (Marusic et al. 2011). It was observed that for relatively low Reynolds number turbulent boundary layer ($Re_\tau \approx 1000$) subjected to the adverse pressure gradient, apart from the inner peak of longitudinal velocity fluctuations u' a second maximum located in the outer zone of turbulent boundary layer appears. It was found that the large-scale motions are much more energetic for adverse pressure gradients compared with the zero gradient case and that the pressure gradient affects mostly the outer region of the flow. Using the method proposed by Mathis et al. (2007), based on correlation function and Hilbert transform, we obtained a clear evidence of a strong correlation between small, inner layer, and large, log layer, structures, which is similar to that observed for zero pressure gradient high Reynolds number cases. A simple model of modulation process occurring in adverse pressure gradient boundary layer has been proposed.

Key words: near wall cycle, inner-outer flow interaction, adverse pressure gradient

INTRODUCTION

Nowadays, it is widely accepted that significant part of wall turbulence consist of the coherent vortical motion or coherent structures. Theodorsen (1952) proposed a model of hairpin vortex, as a simple flow structure that explains existence of the low-speed streamwise streaks inducing the ejection event of the near-wall fluid into higher part of boundary layer. This hairpin vortex consist of two counter rotating vortices (legs) connected with the head inclined to the wall at approximately 45° as it is shown in Fig. 1a. According to Stanislas et al. (2008), such a symmetrical harpin rarely exists and the flow is dominated rather by asymmetrical hairpins. Adrian et al. (2007) proposed the concept of hairpin packet (Fig 1b), according to which a number of hairpins are aligned in the stock in the streamwise direction. In that model long-low speed streak is induced by the heads and between the legs of hairpin vortices. Outside the legs high speed flow regions called sweeps are present. These long low- and high-speed streaks have been observed by Hutchins and Marusic (2007) who call them "superstructure" events. Recently Mathis et al. (2007) have found the existence of coupling between large-scale component of the velocity signal (referring to the superstructure events) and amplitudes of small-scale signal component near the wall within high Reynolds number zero pressure gradient (ZPG) turbulent boundary layers (TBLs), which was called "near wall turbulence production cycle". Their conclusions were formulated based on analysis performed on a single experimental data set extracted from turbulent boundary layer of a high Reynolds number $Re_\tau = \frac{u_\tau \delta}{\nu} = 7300$, where $u_\tau = \sqrt{\frac{\tau_w}{\rho}}$ is friction velocity (τ_w is the wall shear stress, ρ is

flow density), δ is boundary layer thickness and ν kinematic viscosity. Authors showed that, once the pre-multiplied energy spectrum $k_x \Phi_{uu}/{u_\tau}^2$ of streamwise velocity component is analysed, where k_x is streamwise wave number and Φ_{uu} is probability density function of streamwise velocity component spectrum two distinct peaks exist (Fig. 2).. Fig.2 shows that the inner and outer peaks, marked by +, are clearly separated in wave number space. First peak located close to the wall is a footprint of energy originated from low and high speed streaks scaled in viscous units (Kline et al. 1967). Location of this inner peak is invariable in viscous length scale: $y^+ = 15$ and $\lambda_x^+ = 1000$, where y is wall normal coordinate and λ is a length scale in viscous units. The second distinct peak, referred to as the outer peak which according to Mathis et al. (2007), origins from the superstructure type event observed in the log layer. As opposed to the inner peak the location of the last peak scales on the outer scale i.e. boundary layer thickness and equals $y/\delta = 0.05$ and $\lambda_x = 6\delta$.

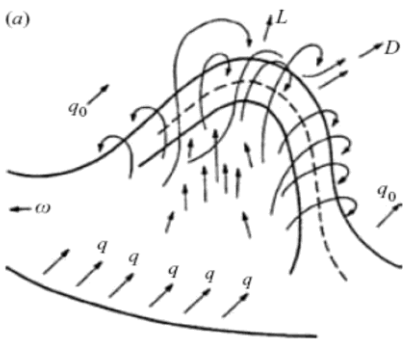

Fig. 1a Theodorsen's hairpin vortex (Theodorsen 1952). The arrows on either side of the hairpin indicate the direction of the flow.

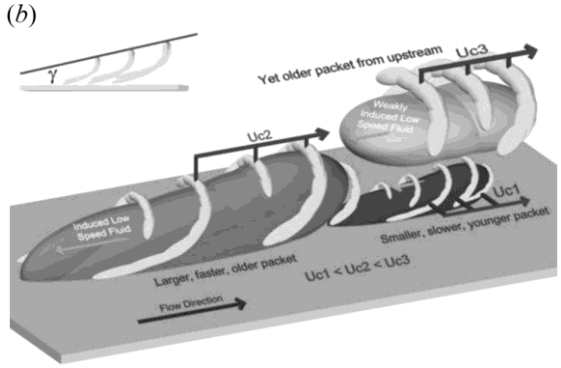

Fig. 1b Very large scale motion model of Adrian et al. (2007) in which hairpin packets align to produce the long, low-momentum streaks.

It was proved (Mathis et al. 2007) that appearance of that outer peak has a direct connection with the coupling process present in the buffer layer for $Re_\tau \gtrsim 1700$. It also coincidences with energy increase in log region. That phenomenon was not observed for lower Reynolds numbers, because of insufficient separation of the inner and outer peak scales. Further study of Marusic et al. (2011) shows that with the increase of Reynolds number the outer peak on the pre-multiplied energy spectra enhances and the coupling process between scales is stronger in the buffer layer. It leads to conclusions that large-scale component play an important role in the high Reynolds number wall bounded flows and could have important implications in the active control of turbulence such as reduction of drag or increase of lift force.

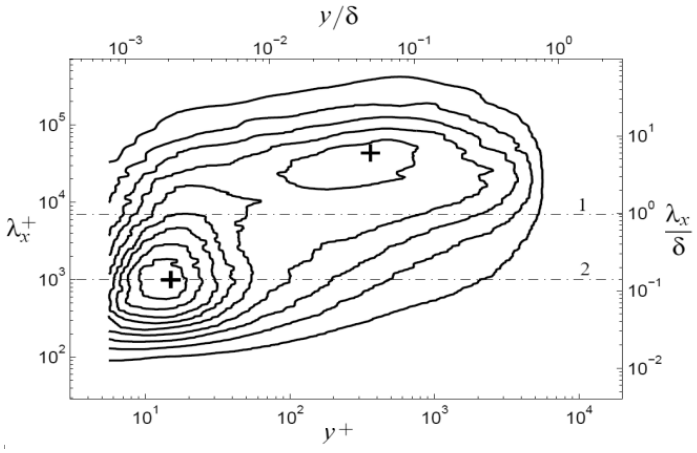

Fig. 2 Iso-contours of the pre-multiplied energy spectra of streamwise velocity fluctuation $k_x\Phi_{uu}/u_\tau^2$; Contour levels are form 0.2 to 2.0 in steps of 0.2. The large "+" mark the inner peak ($y^+ = 15$, $\lambda_x^+ = 1000$) and the outer peak ($y/\delta = 0.05$, $\lambda_x/\delta = 6$); The horizontal dot-dashed lines show the location of the spectral filters (Mathis et al. 2007).

From a practical point of view the more important is the knowledge about the coupling between scales in the turbulent boundary layer under the impact of pressure gradient and especially adverse pressure gradient (APG). Motivation to the present paper was build upon the investigations of the mean flow under APG conditions performed by Materny et al. (2008), and analysis of bursting structures behavior in APG region of this flow by Dróżdż et al. (2011) and Dróżdż & Elsner (2011). Aim of present work is to study the coupling process between large-scale log region motions and the near wall turbulence production cycle in zero and adverse pressure gradient turbulent boundary layer at lower Reynolds number than it was investigated by Marusic et al. (2011).

EXPERIMENTAL SETUP

To investigate the effect of the coupling between large- and small-scales in the TBL under APG conditions an experimental study has been undertaken. The measurements of the velocity field using the single wire probe were performed in an open-circuit wind tunnel, where the TBL developed along the flat plate, which was 2807 mm long and 250 mm wide. The upper wall of test section was shaped according to the assumed distribution of pressure gradient corresponding to the conditions encountered in axial compressor blading (Fig. 3b). The velocity at the inlet plane outside the boundary layer was 15 m/s, while the turbulence intensity equals $Tu = 0.4$ %. Tripping of boundary layer, after the flat plate leading edge, allowed to obtain value of Reynolds number $Re_\tau \approx 1000$. For the purpose of current investigations two cross-sections were selected. First one located in zero pressure gradient region ($Sg = 0.185$) and second one located in adverse pressure gradient region ($Sg = 0.597$), where the pressure parameter $\beta = \frac{\delta^*}{\tau_w}\frac{dP_\infty}{dx}$ is equal 4.1 (where δ^* is displacement thickness and P_∞ is static pressure of the free stream). The cross-sections in the region of APG flow is located slightly downstream the maximum of APG (see Fig. 3b). The locations of the cross-sections are shown in Fig. 3 by black dashed lines. The velocity measurements were done with the modified single wire probe (Dantec Dynamics 55P31) of a diameter $d = 3\mu$m and length in viscous units $l^+ < 20$. The single wire probe was combined with the DISA 55M hot-wire anemometer connected to 14 bit PC card. Acquisition was maintained at frequency 50k Hz with 10 seconds sampling records.

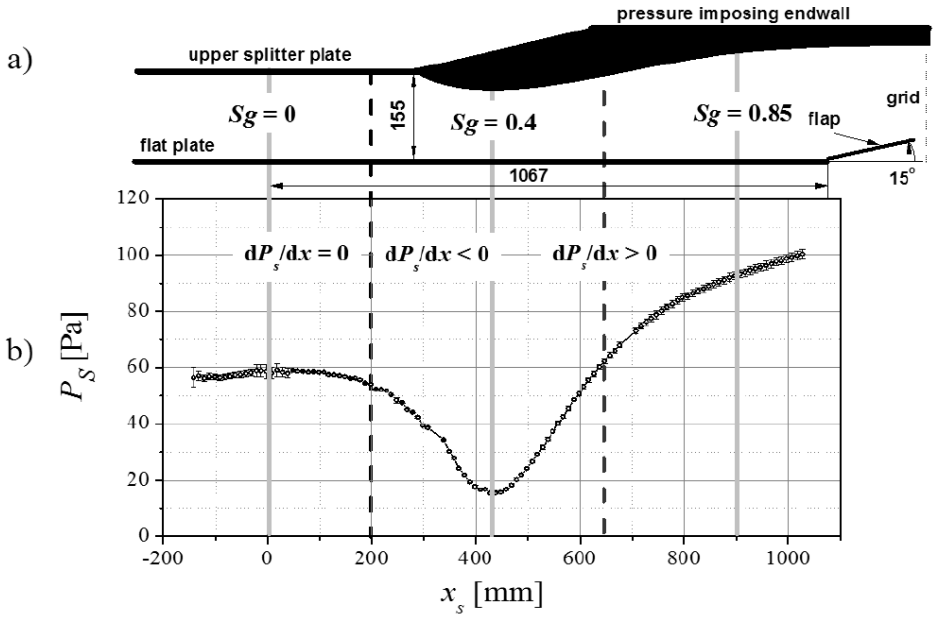

Fig.3. The view of test section a), corresponding static pressure distribution along the plate b).

FLOW CHARACTERISTICS

Studies presented by Materny et al. (2008) showed, among the other, that for the low Reynolds number flow, $Re_\tau \approx 1000$, under APG conditions the similar outer peak to that which was observed for high Reynolds number ZPG boundary layer is noticed. Its presence suggests a strong coupling between large and small scales. Analysis of the mean flow quantities of the TBL under APG preformed by the Materny et al. (2008) shows that the near-wall region grows much more slowly than the outer part of the boundary layer, what in turn implies that most contribution to boundary layer growth originates from region located far from the wall. It was confirmed by the appearance of the outer peak of fluctuations, located in the range of $y^+ = 100 \div 300$, which drives the downstream development of TBL.

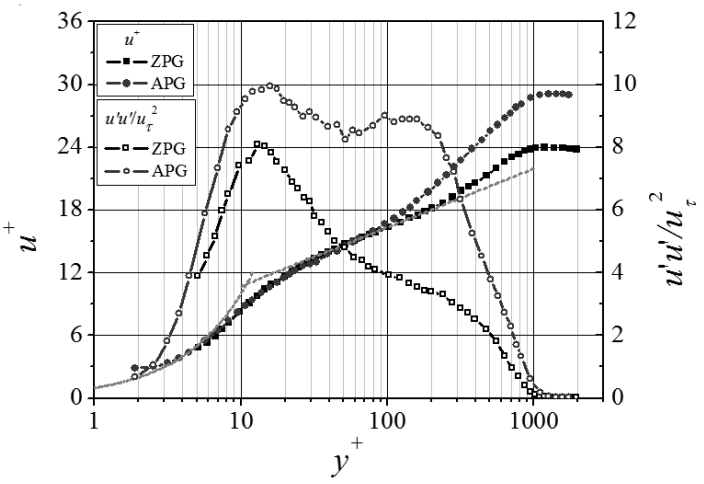

Fig. 4. Velocity profiles and normal $u'u'$ Reynolds stresses in the viscous units at ZPG and APG regions of TUCz experiment. u' - fluctuationg streamwise velocity.

Fig. 4 presents the mean velocity profile u^+ and Reynolds stresses of the $u'u'$ for two chosen cross-sections from ZPG (grey) and APG (dark) conditions. One can observe the significant difference between these two cases. Profile of the mean velocity in the APG region is different from the well known for ZPG flows. In particular, the difference is observed in the wake region as a positive shift of u^+. For APG flow apart from the well known inner peak of $u'u'$ located at $y^+ \approx 15$ the apparent outer peak is observed at the location of $y^+ \approx 120$. Magnitude of this peak is barely the same as the inner one and constantly increases in the viscous unit downstream the flow, what is not shown, however, in the graph. It indicates the possibility of appearance of the outer scale peak in the energy spectrum. Therefore the first task was to analyse and compare the energy spectra for ZPG and APG flows in the wider range of scales. In order to estimate the energy distribution for the defined range of scales the energy spectrum using wavelet transformation was calculated for number of points across the boundary layer thickness. To obtain the wavelet transform of the each recorded signal a Mexican Hat wavelet function was used. According to Gordeyev such a wavelet function is the best choice to perform the analysis of the single events in the time signal.

Iso-conturs of the wavelet energy spectra E_W, scaled by the friction velocity, as a function of the y^+ are presented in Fig. 5. The left set of figures (Fig 5a and c) presents spectra as a function of the length scale λ^+, while the right set of figures (Fig 5b and d) as a function of the time scale, both in viscous units. In order to transform between these two kinds of scales the mean local velocity was used. First peak corresponding to the small-scale component is clearly visible for the both locations while the outer peak exist only for APG flow region (Fig 5c and d) at location $y/\delta = 0.12$ for the length scale $\lambda_x = 1 \div 2\delta$. Despite the scale separation of the inner and outer peak is relatively small the outer peak for $y^+ = 120$ clearly appears for APG flow. It can be assumed therefore that it is a similar phenomenon to that observed by

Mathis et al. (2007) To confirm that assumptions it was decided to perform analysis aimed to detect interaction between large log layer and small inner layer scales.

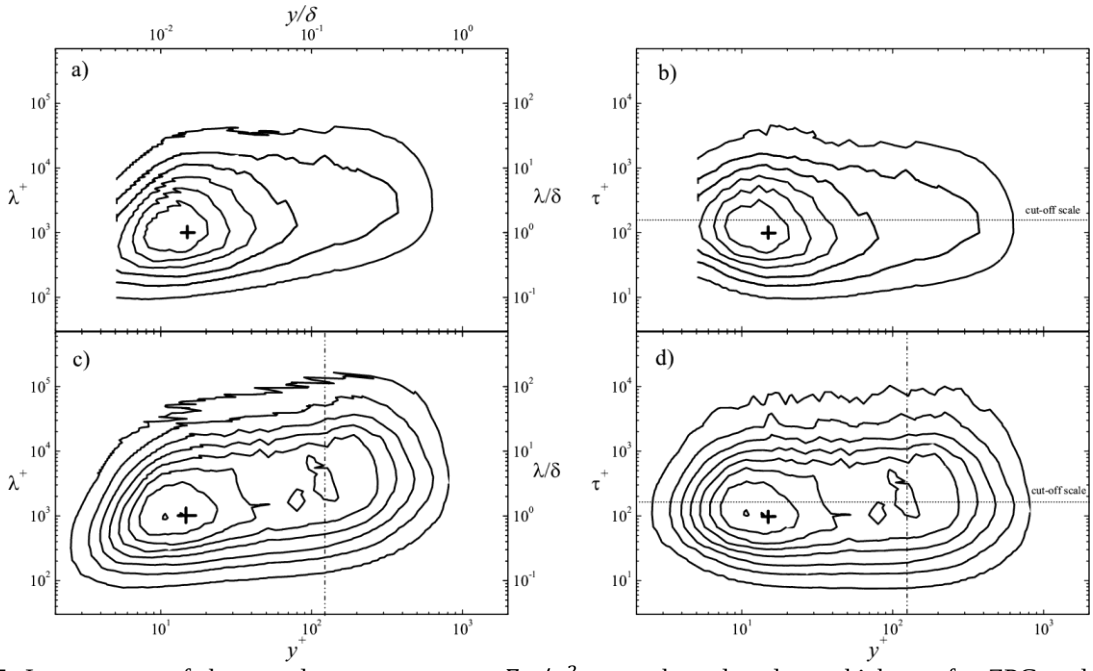

Fig. 5. Iso-contours of the wavelet energy spectra E_W/u_τ^2 across boundary layer thickness for ZPG and APG conditions ($Sg = 0.185$, $Sg = 0.597$) in function of: a) length scale (ZPG); b) time scale (ZPG); c) length scale (APG); d) time scale (APG). Contour levels are from 0.3 to 2.4 in steps of 0.3. "+" points the inner peak location ($y^+ = 15$, $\lambda_x^+ = 1000$). The horizontal dot lines show the location of the spectral filter, while vertical dot-dashed lines shows the location of the outer peak in the APG flow ($y/\delta = 0.12$, $\lambda_x/\delta = 1 \div 2$).

METHODOLOGY

In order to study the coupling process the method proposed by Mathis et al. (2007) was used. This method utilises the correlation function of the single velocity signal, which has to be specially processed. Velocity signal is decomposed onto small and large scale components using high and low pass filtration. During the first step the filtered small-scale component has to be specially prepared in order to obtain the envelope of the signal amplitude. In order to extract not only the information about the amplitude but also about the derivative of the signal the small-scale component u_s has to be additionally processed by the Hilbert transform:

$$H\{u_s\} = \frac{1}{\pi}\int_{-\infty}^{+\infty} \frac{u_s(\tau)}{t-\tau}\, dt. \tag{4.1}$$

One important property of the Hilbert transform is:

$$H\{\cos(t)\} = sin(t), \qquad H\{\sin(t)\} = -cos(t). \tag{4.2}$$

Now the envelope of the amplitude of the signal and its derivative can be calculated by the following equation:

$$E = \sqrt{(u_S)^2 + (H\{u_S\})^2}\,. \tag{4.3}$$

Envelope provides information about amplitudes of both the velocity signal and the Hilbert transform of the small-scale component. The results of the above procedure is presented in Fig 6.

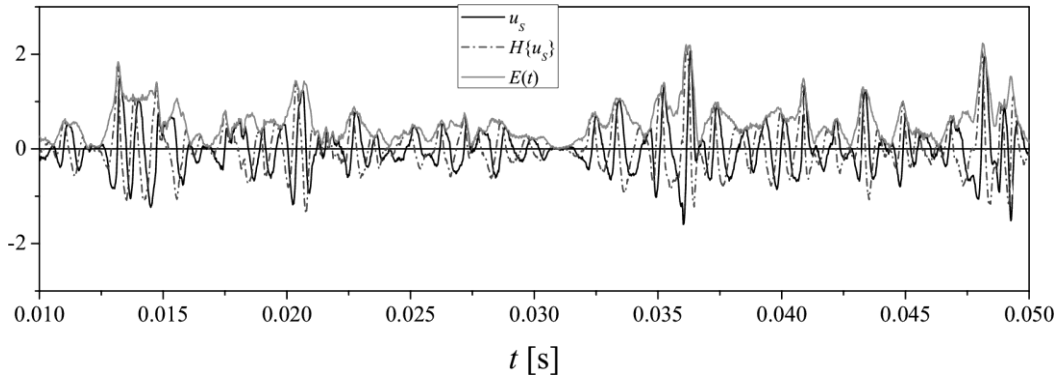

Fig. 6 Time traces of the small-scale component $u_S(t)$, its Hilbert transform $H\{u_s\}$ and envelope $E(t)$ for ZPG case and $y^+ = 5$.

In order to obtain the correlation between envelope $E(t)$ and large-scale component $u_L(t)$ it is necessary to use the low-pass filter of both signals. The result of this process is showed in Fig. 7. To demonstrate the relationship between both time traces the envelope E_L is gained 3 times and shifted down by constant C, which is mean value of the envelope. As it is shown in Fig. 7 the time traces obtained from the signal recorded in viscous sub-layer of the ZPG flow are qualitatively highly correlated (R = 0.535).

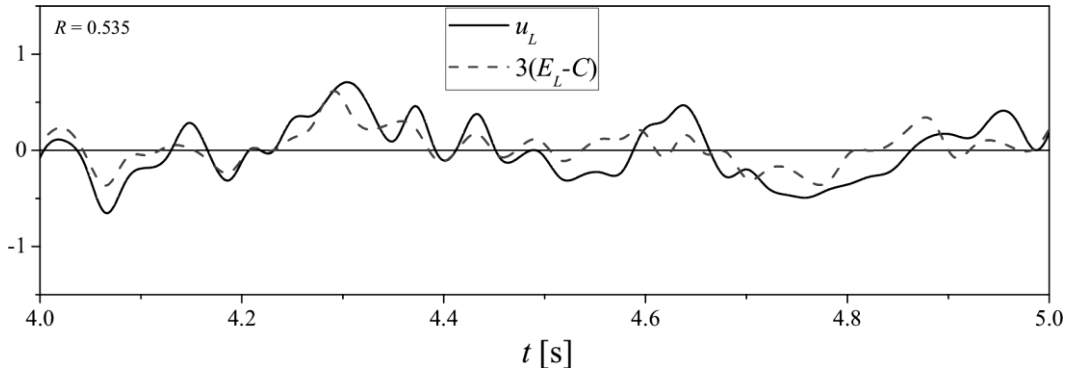

Fig. 7. Time traces of the large-scale component $u(t)_L$, and filtered envelope $E(t)_L$ for ZPG case and $y^+ = 5$.

Correlation coefficient, which is the measure of the modulation of the amplitude of the small-scale component by the large scale-component, was calculated according to equation 4.5:

$$R = \frac{\overline{E_L u_L}}{\sqrt{\overline{E_L}^2}\sqrt{\overline{u_L}^2}}. \tag{4.5}$$

The described above procedure was used for all measuring locations across boundary layer thickness.

RESULTS

The first step of the study was the assessment of qualitative relationship between the small scale and the large scale component recorded at three relative distances from the wall i.e. $y^+ \approx 5, 50, 800$. In order to have small- and large-scales signal components the carrier velocity signal was filtered by high and low pass filtering respectively. The cut-off frequency was set at time scale $\tau^+ \approx$ 160 corresponding to the length scale $\lambda_x{}^+ \approx 1700$, which is located in the middle between the inner and outer peaks. Fig. 8 presents comparison of the coupling between scales for three distances from the wall for ZPG and APG. First location is in the sub layer ($y^+ \approx 5$), second one in the buffer layer ($y^+ \approx 50$) and the third one in the wake region ($y^+ \approx 800$). For each case Fig. 8 presents a carrier signal (upper time trace), large-scale signal

component (middle time trace), while the lower time trace presents the small-scale signal component together with the envelope (dot lines) corresponding to the large-scale signal. The envelopes were shifted in normal direction in order to trace easily the variations of magnitude of small scale component. For the first distance in both cases (Fig. 8a and b) the coupling is evident as the small-scale component signal is clearly modulated by the large-scale motions. For ZPG case, in the buffer layer (Fig. 8c and d), the correlation is very low (Fig. 8c) because the amplitude of the small-scale signal is rather invariant while the envelope changes (empty spaces between small-scale signal and envelope). However, for the APG case (Fig. 8d) small-scale in some extent varies with the envelope. This confirms assumptions about scales modulation in the APG TBL for lower Reynolds number. For the last location (Fig. 8e and f), it is clearly visible that the small-scale component in both cases do not follow the shape of the envelope. As the amplitude of the large-scale component drops the magnitude of small-scale component is enhanced and vice versa. This means that in both cases the small-scale component is inversely correlated with the large-scale component.

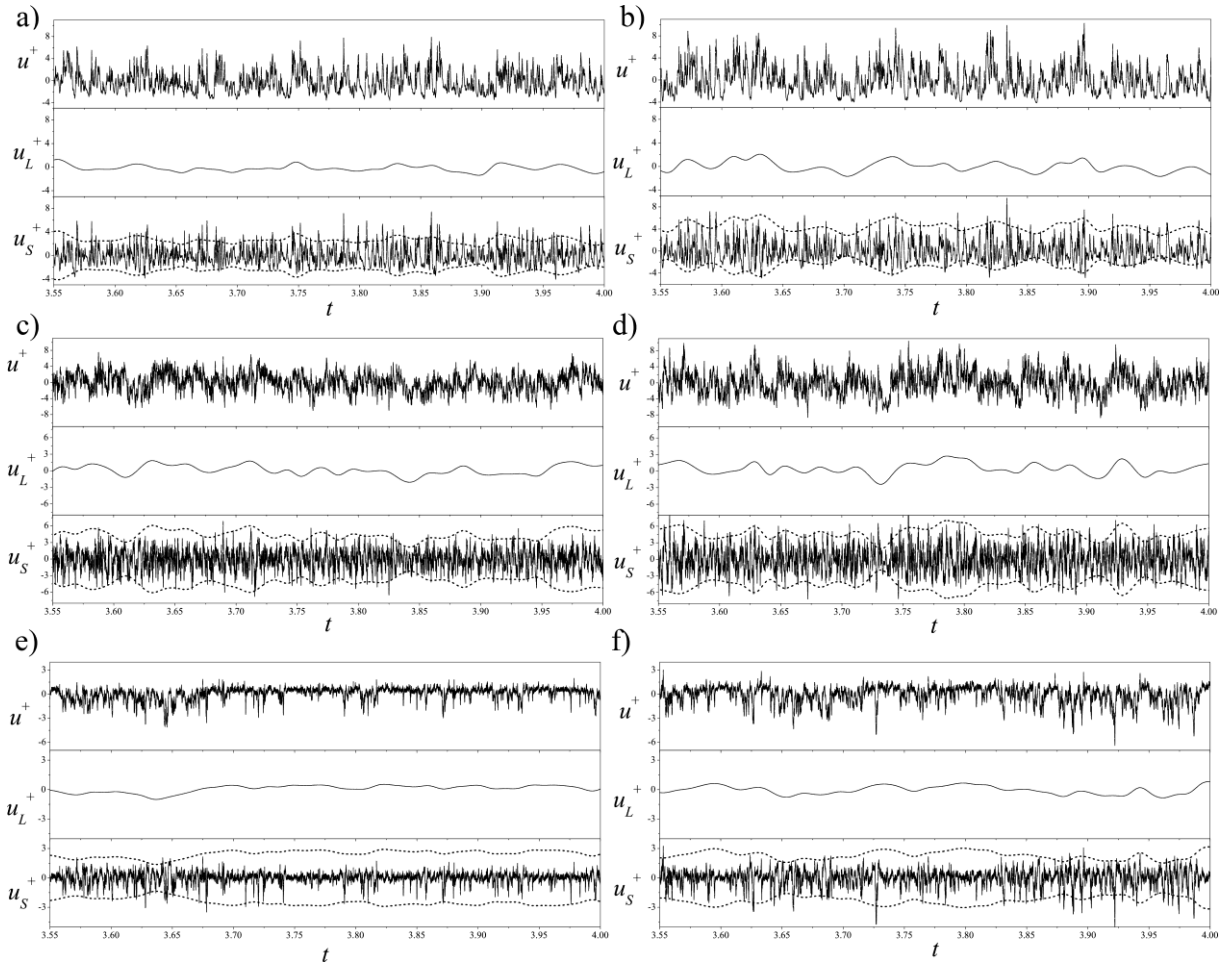

Fig. 8 Visual comparison of the coupling of the scales for three location for ZPG (left a, c, e) and APG (right b, d, f): $y^+ \approx 5$ (a – b), $y^+ \approx 50$ (c – d), $y^+ \approx 800$ (e – f).

The above analysis shows that even for low Reynolds number flow but under APG conditions there is evidence of the modulation phenomenon in the buffer layer. On the other hand for the same Reynolds number under ZPG flow the modulation is marginal. In order to determine the strength of this modulation, the correlation coefficient R across boundary layer thickness was calculated using the equation (4.5). Fig. 9 shows correlation R coefficient distributions for two analyzed cross-sections from ZPG and APG regions. For comparison the literature data taken from Marusic et al. (2011) are presented in Fig. 10.

As it is seen (Fig. 9, 10) the correlation curve R has a characteristic shape with the maximum in viscous sub-layer, the minimum at the edge of boundary layer and a local plateau in the buffer layer. It can be noticed however, that for APG flow the correlation between scales, in that region, is relatively high ($R \approx 0.3$), whereas for ZPG flow it has a value near zero. Literature data (Fig. 10) exhibits also the elevation of R, in the buffer layer, with the increase of Reynolds number. According to Marusic et al. (2011) this region is probably the source location of the modulation. Additionally, the shift of the minimum, at the edge of boundary layer towards higher y^+ values, is observed. It seems that extremes of the correlation function in the viscous sub-layer and at the edge of boundary layer appear regardless of zero or adverse pressure gradients (Fig. 9 and Fig. 10). It is worth noting that intersection of R distribution with y^+ axis in the log layer coincides with the location of the outer peak of $u'u'$ distributions.

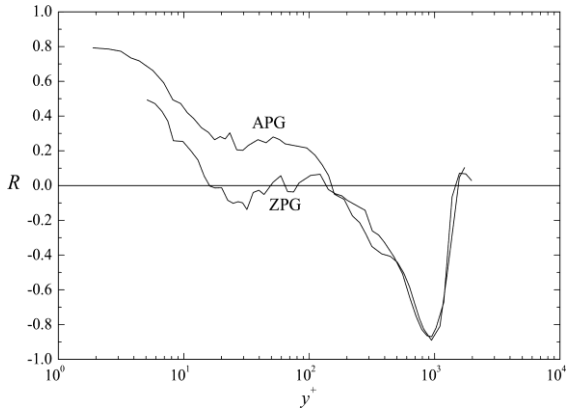

Fig. 9 Wall-normal variation of the degree R of modulation for ZPG and APG conditions at Reynolds number $Re_\tau = 1000$ (CTU)

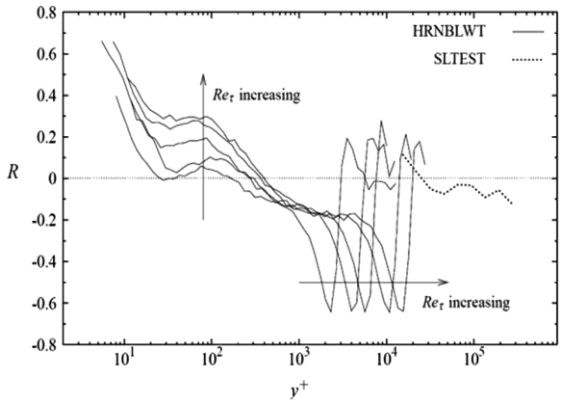

Fig. 10 Wall-normal variation of the degree R of modulation for several Reynolds numbers; $Re_\tau =$ 2800, 3900, 7350, 13600 & 19000 from laboratory facility (HRNBLWT); $Re_\tau = 6.4 \times 10^5$ from atmospheric surface layer (SLTEST) (Marusic et al. 2011)

The reason for the strong correlation near the wall in the APG flow is twofold. On the one hand, structures already formed in packets before APG region, expand under APG conditions and are responsible for the outer peak of $u'u'$ and the modulating effect. On the other hand, the weakening of the inner peak in the APG region (what is not observed for ZPG flows) allows the strong large-scale structures, responsible for the outer peak, to change the momentum near the wall altering the turbulence production. In summary it is worth noting that for ZPG case the shape of R function is similar to that observed in Fig. 10 for the lowest Reynolds number case ($Re_\tau = 2800$). In turn for the APG case (Fig. 9, $Re_\tau = 1000$) the shape is similar to that observed for high Reynolds number flows (Fig. 10, $Re_\tau = 13600, 19000$).

A strong correlation relationship between small and large scale structures, that has been shown, allow to formulate a simple model of modulation process in the APG TBL presented in Fig. 11. Of course due to limited amount of data it could be treated only as a hypothesis, which has to be confirmed by the further study. According to this model the large-scale structure has comparable length scale in the y direction to the boundary layer thickness δ. Occurrence of such a structure has been suggested by Adrian et al. (2007) who has proposed a conceptual scenario of packet of hairpins structures in the outer region of TBL inducing a large scale low speed fluid (see Fig.1b). Hutchins & Marusic (2007) clearly show that the footprint of this large-scale "superstructure" event can extend deep into the near-wall region. In accordance with the principle of mass conservation the other high speed fluid event should appear above this packet. So, the concept of large superstructure vortices, which extend across the whole boundary layer is thus justified (see Fig. 11) The direction of rotation of this

structure is shown by grey arrows. If one can imagine the movement of such a structure in the boundary layer and then divide the area that it occupies in four parts (quadrants), it could be assumed that near the wall the production of small-scale structures is observed in the area IV where the high momentum zone exist. It is confirmed by the time courses (right-hand side plots), where in this region the magnitude of the small-scale fluctuations is consistent with the sign of the large-scale $u_L(t)$ signal, and resulting the positive value of R function. The opposite behaviour occurs in the outer region of TBL (area II), where the negative values of the correlation exist. The temporary velocity deficit above the large-scale structure induced by ejection behind the large-scale vortex center enhances the shear layer at the edge of TBL. This enhanced shear layer could produces the small-scale structures at the edge of TBL. It is confirmed by the time courses (right-hand side plots) that in the outer region the magnitude of the small-scale fluctuations are in opposite phase to the sign of the large-scale $u_L(t)$ signal.

Presented model is different in its assumptions to the model proposed by Marusic et al. (2010) for ZPG flow. Their model explains the coupling between small-scale structures located respectively above and below of the low and high speed quasi-streamwise streaks located in the inner layer. Therefore, their concept is valid only near the wall, and does not explain modulation effects at outer edge of boundary layer. Our model clarifies however the mechanism of the modulation in the whole turbulent boundary layer. Enhancement of amplitude of small-scale component occurs in the area II and IV, while the damping in the area I and III it is shown on the right hand side of the scheme (Fig. 11).

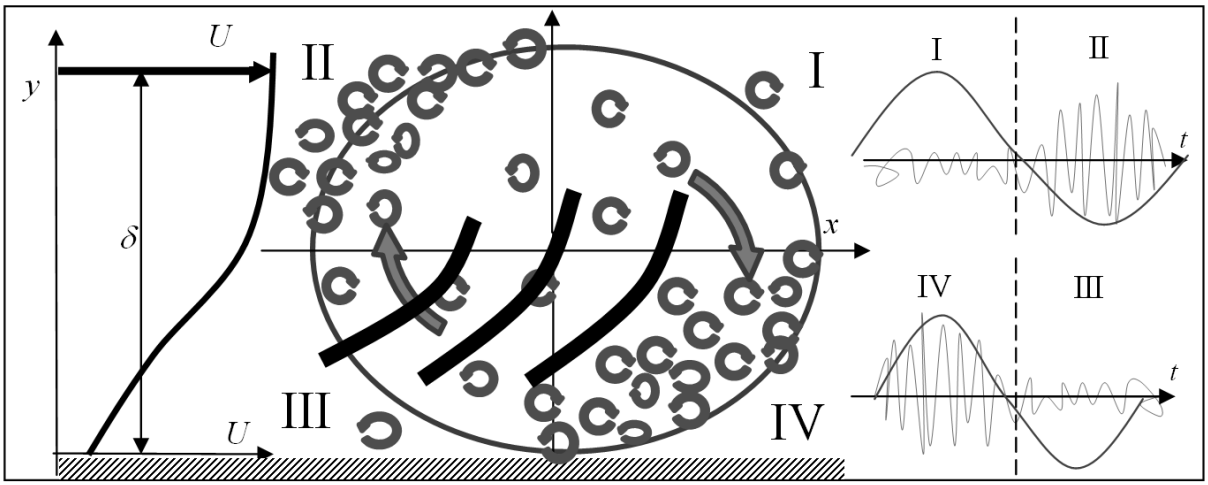

Fig. 11. Scheme of the amplitude modulation of the small-scale component by the large-scale component**.**

The concept of this large scale vortex extending across the boundary layer thickness might also explain the change of movement direction of the small-scale vortices in the APG flows. In the front of the large-scale structure small-scale vortices are swept towards the wall while in the rear part of the structure they are ejected outward the wall. This effect was observed by Dróżdż et al. (2011) and Dróżdż & Elsner (2011), who studied bursting phenomenon in APG turbulent boundary layer. They showed that under APG conditions bursting structures increase the angle of motion with respect to the wall. Conclusion was formulated based on phase averaged $< u >$ and $< v >$ velocity components. Additionally, the analysis of phase averaged fluctuations showed that, in comparison with ZPG, $< u >$ velocity component is much higher than $< v >$ velocity component what also suggest that angle of vortex motion is higher in the APG flow. Based on the present results as well as on data presented Dróżdż and Elsner (2011) one can speculate that the near wall structures are thrown from the wall to the log region by the large-scale structure and that the process is enhanced by APG.

CONCLUSIONS

The influence of the adverse pressure gradient on the near wall turbulence production cycle has been analysed. It was shown that at low Reynolds number APG conditions has highly comparable influence on the near wall turbulence production cycle as high Reynolds number observed for ZPG flow at. It was observed that for relatively low Reynolds number ($Re_\tau \approx 1000$) and adverse pressure gradient, apart from the inner peak of longitudinal velocity fluctuations u' a second maximum located in the outer zone of turbulent boundary layer appears. It was found that the large-scale motions are much more energetic for adverse pressure gradients compared with the zero gradient case and that the pressure gradient affects mostly the outer region of the flow. Using the method proposed by Mathis et al. (2007), based on correlation function and Hilbert transform, we obtained a clear evidence of a strong correlation between small inner layer, and large log layer, structures, which is similar to that observed for zero pressure gradient high Reynolds number cases. Additionally, a simple model of modulation process occurring in adverse pressure gradient boundary layer has been proposed. This model explains also the reason of increased angle of the bursting vortical structures motion observed by Dróżdż and Elsner (2011). The knowledge about the modulation process could be useful to develop new methods of drag reduction in the adverse pressure gradient wall bounded flow, which are often present in many engineering applications.

ACKNOWLEDGEMENTS

The investigation was supported by National Committee for Scientific Research Grant no.: N N501 098238 (2010-2011).

REFERENCES

Adrian, R. (2007): *Hairpin vortex organization in wall turbulence*. Phys. Fluids Vol. 19 (4), 041301.

Dróżdż A. & Elsner W., (2011): *Detection of coherent structures in a turbulent boundary layer with zero, favourable and adverse pressure gradients*, J. Phys.: Conf. Ser., Vol. 318 062007 doi:10.1088/1742-6596/318/6/062007

Dróżdż A., Elsner W. & Drobniak S. (2011): *Application of VITA technique for detection of the organized structures present in a turbulent boundary layer under an adverse pressure gradient*. Arch. Mech. Vol. 63, pp. 183-199.

Gordeyev, S. *POD, LSE and Wavelet decomposition: Literature Review*

Kline, S. J., Reynolds, W. C., Schraub, F. A. and Rundstadler, P.W. (1967): *The structure of turbulent boundary layers*, J. Fluid Mech., Vol. 30, pp. 741–773

Hutchins, N. and Marusic, I. (2007): *Evidence of very long meandering features in the logarithmic region of turbulent boundary layers*, J. Fluid Mech., Vol. 579, pp. 1–28.

Marusic I, Mathis R., Hutchins N., (2011): *Reynolds number dependence of the amplitude modulated near-wall cycle*, Progress in Wall Turbulence: Understanding and modeling, ERCOFTAC Series 14, pp. 105-112.

Marusic I, Mathis R., Hutchins N. (2010): *Predictive Model for Wall-Bounded Turbulent* Flow, Science Vol. 329 no. 5988 pp. 193-196, DOI: 10.1126/science.1188765

Materny M., Dróżdż A., Drobniak S., Elsner W. (2008): *Experimental analysis of turbulent boundary layer under the influence of adverse pressure gradient*. Arch. Mech., Vol.60, 6, pp. 449–466, Warszawa.

Mathis R., Hutchins N., Marusic I. (2007); *Evidence of large-scale amplitude modulation on the near-wall turbulence*.,16th Australian Fluid Mechanics Conference

Stanislas, M., Perret, L. i Foucaut, J.-M. (2008): *Vortical structures in the turbulent boundary layer: a possible route to a universal representation*. J. Fluid Mech. Vol. 602, pp. 327–382.

Theodorsen, T. (1952): *Mechanism of turbulence*. In Midwest Conference on Fluid Mechanics, Second, pp. 1–18.